Simulating and Modeling for Capacitance and Conductance of Parallel-plate Coupler for under Sea Water Applications

Ning Li[1][0000−0002−6772−675X], Kosuke Iguchi[1], Xuefeng Liu[2][0000−0003−4546−1620], and Takeshi Shinkai[1]

[1] Tokyo University of Technology, Tokyo,192-0982, Japan;
lining@stf.teu.ac.jp
https://www.teu.ac.jp
[2] Tokyo Woman's Christian University, Tokyo 167-8585, Japan
https://www.twcu.ac.jp/main/english/index.html

Abstract. This paper analyzes the modeling and characteristics of parallel-plate capacitors for underwater capacitive wireless power transfer (CWPT) systems. Using finite element method (FEM), this paper has simulated the capacitance and conductance in a seawater environment, and derived fitting equations both for capacitance and conductance from the simulation results by using MATLAB. The derived equations are verified by changing the coupler size. For four different sizes, the maximum error percentage for capacitance is 9.18% at the size of 300mm×300mm; and for conductance, all error percentages are less than 4%. The agreement between the simulated results and the ones calculated from the equations proves the validity of the derived equations for both capacitance and conductance.

Keywords: Coupler · Parallel-plate capacitor · Wireless power transfer · Under sea · Finite element method.

1 Introduction

Nowadays, intelligent sensing systems and intelligent robotics attract a lot of attention both from academic and industry [1, 2]. For these systems, power supply becomes a bottleneck for some applications, especially for those operating in environments difficult to access for human beings. To address this problem, wireless power transfer (WPT) is a good candidate to charge the batteries inside the devices or directly transfer power to them.

Capacitive wireless power transfer (CWPT) is one of the wireless power transfer methods for short-distance power transfer, which employs electric fields as the energy transferring medium. Compared to inductive wireless power transfer (IWPT), CWPT offers several advantages including: (1) lower eddy current losses when penetrating metals, (2) lower cost and weight, (3) better misalignment performance, and (4) low EMI and broader safety range [3, 4]. Based on these advantages, CWPT finds its applications in many areas, including electric

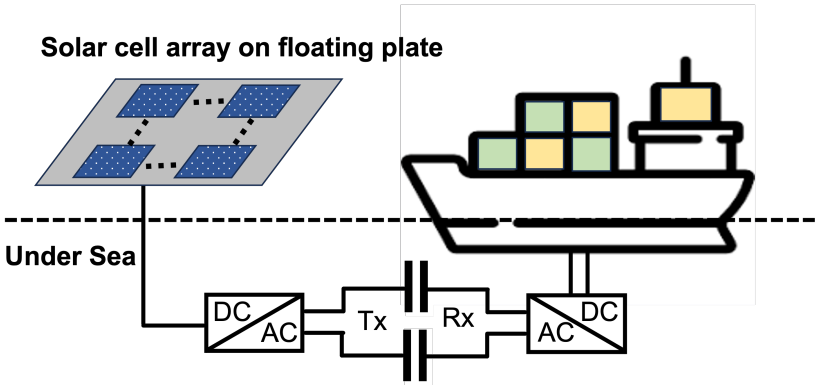

Fig. 1. An application by using capacitive wireless power transfer under seawater. The energy is assumed to be generated by using solar cells on a floating object.

vehicle (EV) charge, dynamic robot wireless power charging, underwater drone wireless power charging and more [5–10]. CWPT is especially beneficial for underwater applications due to the high dielectric constant of water [4, 7–11], even though it has some drawbacks such as low coupling capacitance and low frequency [4]. In these applications, the structure employing two pairs of parallel plates is very common, which act as the electrodes of the power transmitter (Tx) and receiver (Rx) . Figure 1 shows an example application of the four-plate system. A solar-cell system generator is utilized to accumulate solar energy and transfer it to a vehicle.

In the above mentioned application, the performance of the whole power transfer system is usually dominated by the coupler. Therefore, it is important to understand the characteristics of the coupler for the whole system design. With the assumption that the electric field is uniform and perpendicular to the capacitor electrodes, the capacitance of a parallel-plate capacitor can be obtained using the classical equation, $C_{\text{cal}} = \epsilon \frac{A}{d}$, where A is the area and d the distance between two plates. However, the assumption is less accurate due to the electric filed leakage and non-uniformity at the edges.

To increase calculation accuracy, the fringing capacitance needs to be considered. Many works have calculated the fringing capacitance and derived equations accounting for the fringing effect [12–16], These studies deduced the solution of the electric field for a circular parallel-plate capacitor using conformal mapping method. These works perform well for a certain range of parallel round plates sizes.

For square plate-parallel capacitor, it has been analyzed in [17], and an equation has been derived with the consideration of the fringing effect. The authors proposed a general equation with two undefined parameters as shown below,

$$C_{\text{fit}} = C_{\text{cal}}(1 + k_1 \frac{d}{P} ln(k_2 \frac{P}{d})), \tag{1}$$

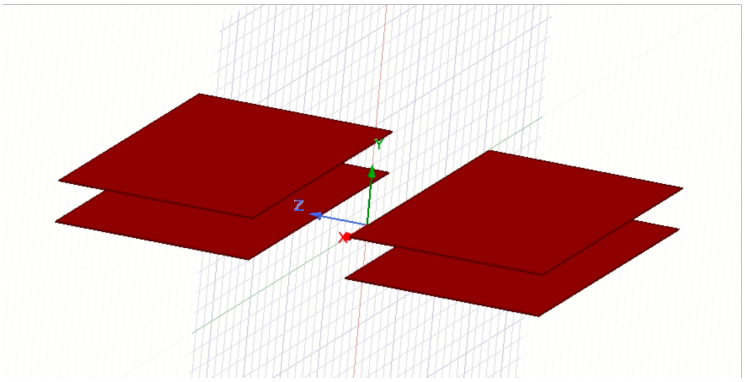

Fig. 2. The schematic of the four-plate conductive coupler in Ansys Maxwell 3D simulator.

where P is defined in [16] as a dimension characteristic of the width of the electrode, such as the diameter of a disc. k_1 and k_2 are the undefined parameters. They determined the values of k_1 and k_2 by employing the finite element method (FEM). More accurate calculation results are obtained by Xu group in [17] compared with former works [12–16]. The reason is that some approximation has been made during derivation of the formulas obtained using conformal mapping in former works.

The above previous works have focused on the analysis of the capacitance in air, and seldom considered the conductance. For underwater applications, due to the high conductivity of seawater, it is necessary to analyze both the capacitance and the conductance, as shown in Fig. 1. Due to its accuracy, the method in [17] is utilized to analyze the coupler under seawater.

This paper is organized as the following: Section II describes the simulation setup for CWPT using the Ansys Maxwell 3D simulator. Section III demonstrates the simulation results, and presents a fitting equation for both the capacitance and conductance with respect to distance. The fitting results are compared with the simulation and calculation ones from classical equations in Section III. The final conclusion is drawn in Section IV.

2 Simulation Setup and Results

2.1 Simulation Schematic and Equivalent Circuit

The simulation schematic is shown in Fig. 2. Four-plate system is employed since it is the most commonly used system in CWTP as mentioned previously. The material for the plates is copper, which has a conductivity of 5.8×10^7 S/m. The design parameters are shown in Fig. 3, and the default values listed in Table 1 are used in the simulation. A region box represents the circumstance around the coupler, which is also shown in Fig. 3. For underwater application, the region is

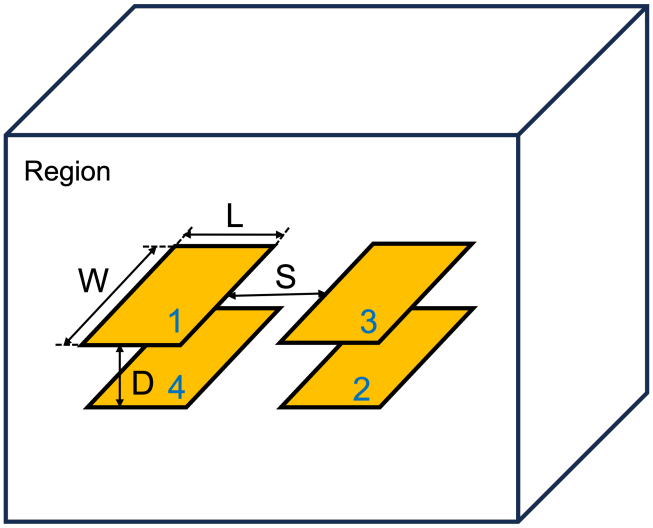

Fig. 3. The whole simulation setup including region and parameters defined for the four-plate conductive coupler.

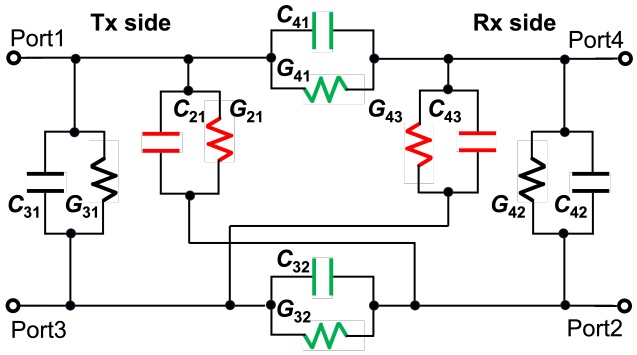

Fig. 4. The equivalent circuit for the four-plate conductive coupler.

Table 1. Default Value of Design Parameters in Fig. 3

Design parameter	Width (W)	Length (L)	Distance (D)	Space (S)	Thickness (T)
Default Value (mm)	180	100	20	50	0.5

set to seawater, which has a permittivity, ϵ_r, of 84, a conductivity, σ, of 4 S/m, and a dielectric loss tangent, $tan(\delta)$, of 0.005 at very low frequency.

Due to the high conductivity of sea water, an equivalent circuit shown in Fig. 4 is considered [18]. The coupling capacitors and conductors between the

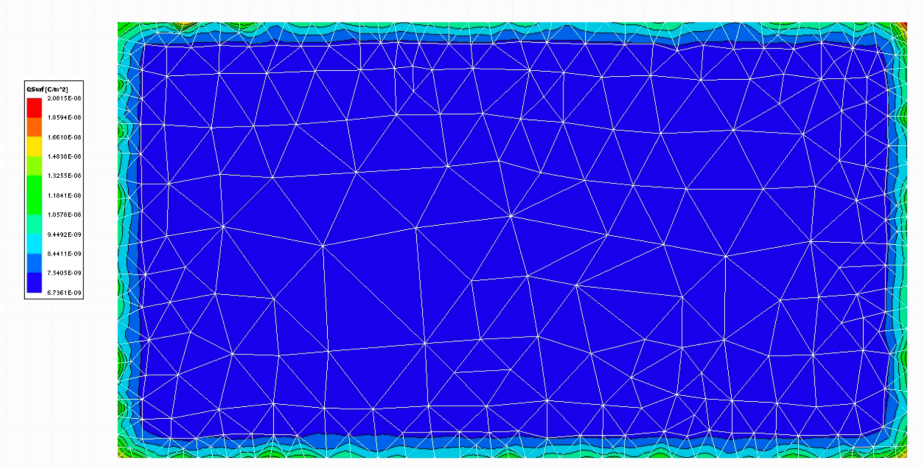

Fig. 5. The distribution of surface charge and mesh on the excitation plate.

Tx and Rx are C_{41}, C_{23} and G_{41}, G_{23}, respectively. The cross capacitors and conductors are given by C_{21}, C_{43} and G_{21}, G_{43}, which are harmful and degrade the power transfer efficiency greatly [8]. The side capacitors and conductors are C_{31}, C_{42} and G_{31}, G_{42}. For system symmetry, we have

$$C_{41} = C_{32}, G_{41} = G_{32}, \tag{2}$$

$$C_{31} = C_{42}, G_{31} = G_{42}, \tag{3}$$

and

$$C_{21} = C_{43}, G_{21} = G_{43}. \tag{4}$$

2.2 Simulation Results

The simulation conditions using Ansys Maxwell 3D have been discussed in [18]. In this paper, the same settings are employed for all simulations. The effect of the relative region size is set to 500 mm, and the adaptive frequency is set to 3 Hz for AC conduction solution. The simulated capacitance and conductance are summarized in Table 2 at the default values listed in Table 1.

For C_{41} and G_{41}, the calculated values are 645 pF and 3.60 S using classical equations $C_{\text{cal}} = \epsilon \frac{WL}{D}$ and $G_{\text{cal}} = \sigma \frac{WL}{D}$, respectively. Compared with the simulated values, the calculated vales are smaller and the error percentage are 29.5% and 29.4% for capacitance and conductance, respectively. The surface charge distribution is shown in Fig. 5. It is evident that the surface charge distribution is not uniform and the density at the edges is higher. This contributes to the non-uniform electric field and difference between the simulated result and the calculated one from classical equation.

Table 2. Simulated Capacitance and Conductance at Default Value of Design Parameters listed in Table 1

.

Capacitance & Conductance	C_{41}	C_{31}	C_{21}	G_{41}	G_{31}	G_{21}
Simulated values	835 pF	123 pF	92.7 pF	4.66 S	0.688 S	0.517 S

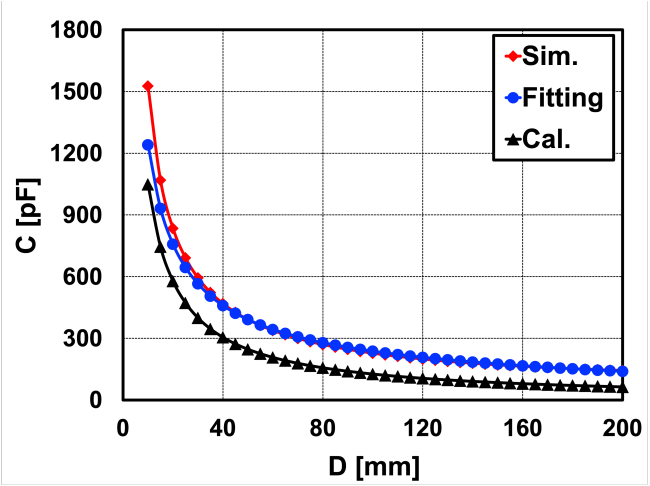

(a)

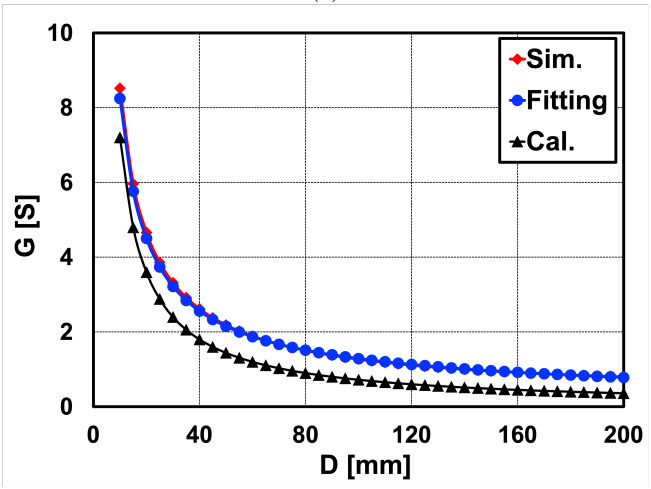

(b)

Fig. 6. Capacitance and conductance variance with respect to D. (a) Capacitance C_{41}. (b) Conductance G_{41}.

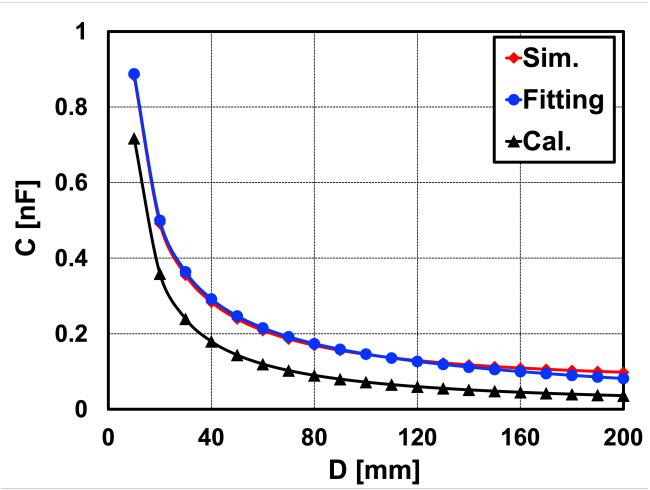

(a)

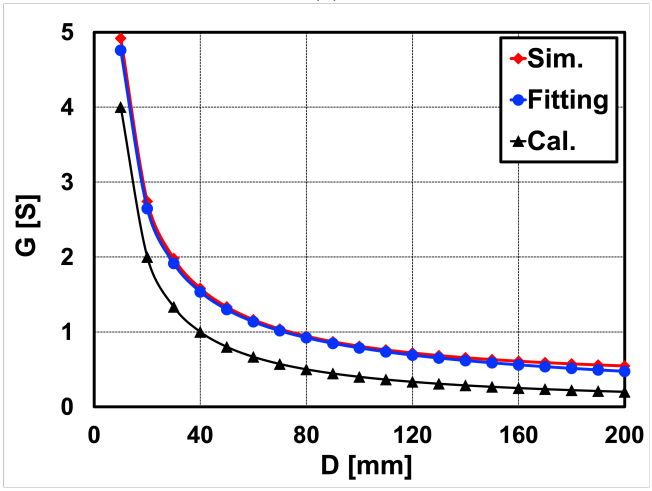

(b)

Fig. 7. Capacitance and conductance variance with respect to D for plate size of 100mm×100mm. (a) Capacitance C_{41}, (b) Conductance G_{41}

3 Modeling and Confirmation for Conductive Coupler

3.1 Capacitance and Conductance Modeling

In the following, fitting equations will be derived for both the capacitance C_{41} and conductance G_{41} for design flexibility. To obtain the model data, firstly the capacitance and conductance variance with distance are simulated using Ansys Maxwell. Next, the simulated data is used to derive the fitting equation in MATLAB by solving linear equations. The fitting equation for capacitance is the same

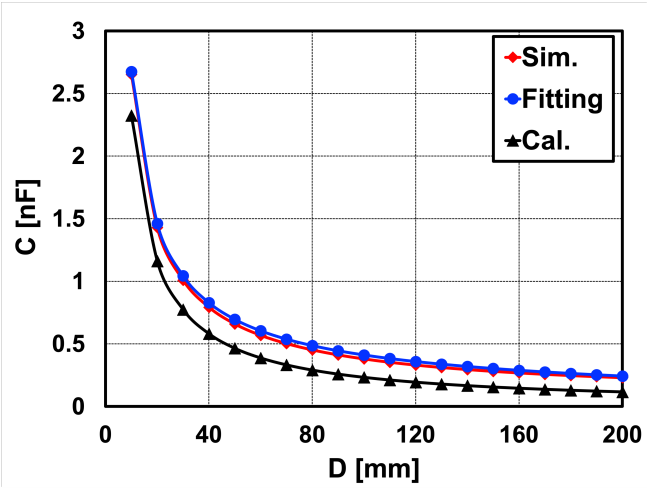

(a)

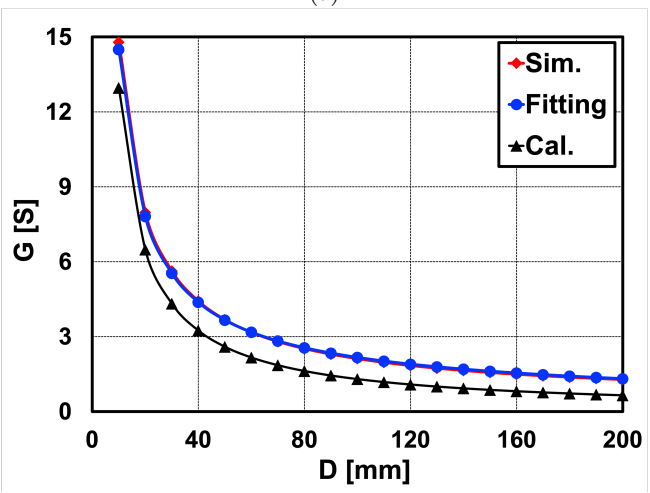

(b)

Fig. 8. Capacitance and conductance variance with respect to D for plate size of 180mm×180mm. (a) Capacitance C_{41},(b) Conductance G_{41} .

as outlined in [17] and given by Eq. 1. As mentioned in [16], the definition and estimation of the parameter P will limit the utility of the equation, particularly for electrodes of irregular shape. Deviating from [16, 17], the parameter P in our works is defined as $2(W + L)$, based on the consideration that the fringing capacitance is usually related to the edge length [16].

The estimated value by employing MATLAB for k_1 and k_2 in Eq. 1 is about 2.33 and 1.49, respectively. The fitted capacitance of C_{41} by using Eq. 1 is compared with the simulated and the calculated ones in Fig. 6(a). Except for

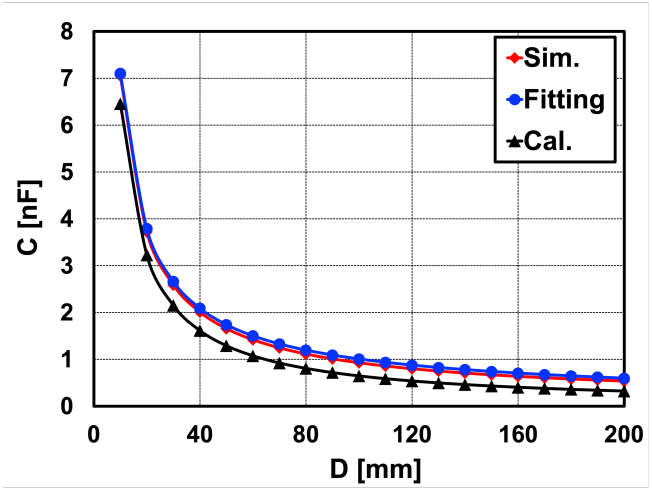

(a)

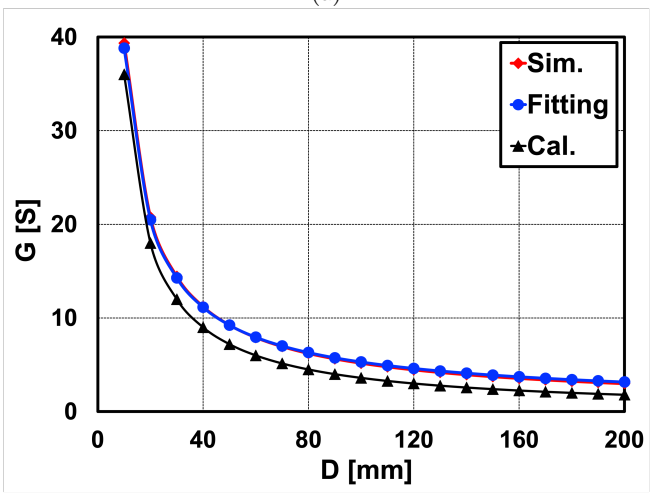

(b)

Fig. 9. Capacitance and conductance variance with respect to D for plate size of 300mm×300mm. (a) Capacitance C_{41}, (b) Conductance G_{41}.

the very narrow distance less than 15 mm, good match is observed across all other distances. The good fitting results is considered resulting from the definition of the parameter P, which is the only difference from other works.

The simulated conductance G_{41} with distance is shown in Fig. 6(b), G_{41} demonstrating a gradual decline as the distance increases, since G is inversely proportional to the distance which can be known from the classical equation. The simulated values are also larger compared to the calculated ones. The difference, similar to the fringe capacitance, we named it as "the fringe conductance". Based

on the same consideration, a mathematical fitting equation in a similar form is also built for the conductance. And to the best of the authors' knowledge, this is the first time that the conductance has been fitted based on the simulation results for underwater capacitors. The fitting equation is given by Eq. 5. α_1 and α_2 are the fitting parameters, with a value of 1.6189 and 2.7206, respectively.

The difference between the fitting results and the simulation is considered coming from the first-order approximation. Implying higher-order approximation equation will decrease the difference, however, the complexity of the fitting equation will increase.

$$G_{\text{fit}} = G_{\text{cal}}(1 + \alpha_1 \frac{D}{P} ln(\alpha_2 \frac{P}{D})). \tag{5}$$

3.2 Verification

Table 3. Plate Size and Error Percentage between the Simulated Results and Those Calculated from Fitting Equation at $D = 20\ mm$

.

Figure No.	W (mm)	L (mm)	Error (%) @ $D = 20\ mm$ for C & G
Fig. 6	180	100	9.18 & 3.34
Fig. 7	100	100	1.76 & 3.49
Fig. 8	180	180	2.20 & 1.99
Fig. 9	300	300	1.83 & 1.37

To further investigate the fitting equations, simulations for couplers with different sizes are carried out using the same method. The simulated values are compared with the calculated ones from the derived fitting equations. The results are shown in Fig. 7, Fig. 8, and Fig. 9. The coupler sizes and error percentages are summarized in Table 3. As can be seen from Table 3, the maximum error percentage for capacitance is 9.18% at the size of $300\times300\ mm^2$ at a distance of 20 mm; while for other sizes, the error percentages are less than 2.20%. For conductance, all error percentages are less than 4%. It is fair to say that the fitting equation works well in all cases.

4 Conclusions

This paper analyzes the modeling and characteristics of parallel-plate capacitors for underwater capacitive wireless power transfer (CWPT) systems. Using finite element method (FEM), this paper has simulated the capacitance and conductance in a seawater environment, and derived fitting equations for both capacitance and conductance from the simulation results by using MATLAB.

This is the first time to derive a fitting equation for the conductance of undersea capacitors. The derived equations are verified by changing the coupler size. For four different sizes, the maximum error percentage for capacitance is 9.18% at the size of 300mm×300mm; and for conductance, all error percentages are less than 4%. The agreement between the simulated results and the ones calculated from the equations proves the validity of the derived equations for both capacitance and conductance.

Acknowledgments. This work was partially supported by Research Center for the Future of Food and Agriculture, Tokyo University of Technology.

Disclosure of Interests. The authors have no competing interests to declare that are relevant to the content of this article.

References

1. Mahmood, M.F., Mohammed, S.L., Gharghan, S.K., Al-Naji, A., Chahl, J: Hybrid Coils-Based Wireless Power Transfer for Intelligent Sensors. Sensors **20**(9), 2549 (2020)
2. Feng, H., Cai, T., Duan, S., Zhao, J., Zhang, X., Chen C.: An LCC-Compensated Resonant Converter Optimized for Robust Reaction to Large Coupling Variation in Dynamic Wireless Power Transfer. IEEE Transactions on Industrial Electronics **63**(10), 6591-6601 (2016)
3. Liu, C., Hu, A.P.: Steady state analysis of a capacitively coupled contactless power transfer system. In: 2009 IEEE Energy Conversion Congress and Exposition. pp. 3233–3238 (2009)
4. Erel, M.Z., Bayindir, K.C., Aydemir, M.T., Chaudhary, S.K., Guerrero, J.M.: A comprehensive review on wireless capactive power transfer technology: Fundamentals and applications. IEEE Access **10**, 3116–3143 (2022)
5. Zhang, H., Lu, F., Hofmann, H., Liu, W., Mi, C.C.: A four-plate compact capacitive coupler design and lcl-compensated topology for capacitive power transfer in electric vehicle charging application. IEEE Transactions on Power Electronics **31**(12), 8541–8551 (2016)
6. Lu, F., Zhang, H., Mi, C.: A two-plate capacitive wireless power transfer system for electric vehicle charging applications. IEEE Transactions on Power Electronics **33**(2), 964–969 (2018)
7. Urano, M., Ata, K., Takahashi, A.: Study on underwater wireless power transfer via electric coupling with a submerged electrode. In: 2017 IEEE International Meeting for Future of Electron Devices, Kansai (IMFEDK). pp. 36–37 (2017)
8. Vincent, D., Williamson, S.S.: Modeling, analysis, design, and verification of a reduced model capacitive power transfer based wireless charging system. In: 2020 IEEE Energy Conversion Congress and Exposition (ECCE). pp. 4118–4123 (2020)
9. Mahdi, H., Hoff, B., Østrem, T.: Evaluation of capacitive power transfer for small vessels charging applications. In: 2020 IEEE 29th International Symposium on Industrial Electronics (ISIE). pp. 1605–1610 (2020)
10. Tamura, M., Murai, K., Matsumoto, M.: Design of conductive coupler for underwater wireless power and data transfer. IEEE Transactions on Microwave Theory and Techniques **69**(1), 1161–1175 (January 2021)

11. Kodeeswaran, S., Nandhini Gayathri, M., Kannabhiran, A., Sanjeevikumar, P.: Design and performance analysis of four plates capacitive coupler for electric vehicle on-road wireless charging. In: 2021 24th International Symposium on Wireless Personal Multimedia Communications (WPMC). pp. 1–6 (2021)
12. Ignatowsky, W.v.: Über doppelpolige Lösungen der Wellengleichung. Berlin (1932)
13. LOVE, E.R.: The electrostatic field of two equal circular co-axial conducting disks. The Quarterly Journal of Mechanics and Applied Mathematics **2**(4), 428–451 (1949)
14. Hutson, V.: The circular plate condenser at small separations. Mathematical Proceedings of the Cambridge Philosophical Society **59**(1), 211–224 (1963)
15. Hughes, B.D.: Comment on the potential due to a circular parallel plate capacitor. Journal of Physics A: Mathematical and General **17**(6), 1385–1386 (1984)
16. Sloggett, G.J., Barton, N.G., Spencer, S.J.: Fringing fields in disc capacitors. Journal of Physics A: Mathematical and General **19**(14), 2725–2736 (1986)
17. Chen, X., Zhang, Z., Yu, S., Zsurzsan, T.G.: Fringing effect analysis of parallel plate capacitors for capacitive power transfer application. In: Proceedings of 4th IEEE International Future Energy Electronics Conference. pp. 1–5 (2019)
18. Li, N., Iguchi, K., Liu, X., Shirane, A., Okada, K., Shinkai, T.: Conductive and capacitive properties of couplers under seawater for electric wireless power transfer. In: 2024 IEEE Wireless Power Technology Conference and Exrpo (WPTCE2024). pp. 1–4. Kotyo, Japan (2024)